# Flux Modelling of Reluctance Machines with Bulk Superconducting Materials

**Athanasis Sfetsos, Murta Pina, Anabela Gonçalves, Ventim Neves, Leão Rodrigues**

Department of Electrical Engineering
Faculty of Science and Technology
New University of Lisbon
2829 - 516 Caparica, PORTUGAL
Teleph: +351 21 294 8545 Fax: +351 21 294 8532
Email: ts@uninova.pt and leao@uninova.pt

***Abstract*** - This paper discusses the finite element modelling of reluctance machines that contain bulk domains of high temperature superconducting (HTS) material. The modelling is performed using a two-dimensional finite element tool, which estimates the flux and current distributions in the various parts of the machine. The HTS elements act as flux barriers and direct the flux inside the material along a predetermined path, improving its performance.

## 1. Introduction

Since the early 1970's there has been considerable effort made to discover the optimal incorporation of low temperature superconducting materials into electric machines. Superconductivity is characterized by extremely low resistivity values and the ability to carry currents several orders of magnitude greater than conventional copper wires. The introduction of these materials into large machines would provide an advance in terms of efficiency, annual savings, weight, volume, and performance characteristics.

Initially the efforts to manufacture superconducting motors failed because of the extremely high cost of liquid helium, the only available coolant for the temperature required to allow type I superconductors.

The discovery of the YBCO compound provided the needed breakthrough, since cooling could be then be achieved using liquid nitrogen, a commonly available and far cheaper coolant. Many prototype machines were built in an attempt to determine the optimal machine that best suits the selected application and its finer characteristics [1].

Two different options exist for the incorporation of HTS materials in electric machines. The first is to use superconductive wires as armatures and coils as a replacement to conventional copper wires to allow the transport of large currents. The second option is to utilize these materials as flux barriers that can direct the magnetic flux inside the machine along a more preferable path and reduce flux leakage. The former option is exploited in synchronous machines.

Finite element analysis is widely used as a modelling tool for the optimisation of the design of electric machines.

Finite element analysis is widely used as a modelling tool for the optimisation of the design of electric machines and there are many commercially available software packages. However, the development of modelling tools that include HTS materials proved a difficult task because there is no solid theoretical background, despite the efforts of the research community, and the additional calculations for these materials result in an increased computational effort.

The object of this work is the modelling of different types of reluctance machines, performed using the Finite Element software developed at the Department of Engineering, Oxford University. The program calculates the magnetic flux in the machine and the induced current distribution in the superconducting pieces. A comparison of the operation of the machine with and without superconducting materials can be made directly, and furthermore conclusions on the optimal machine design can be drawn.

The following sections present an introduction to the principles of superconductivity and finite elements as a modelling tool. The rest of the paper discusses the modelling of reluctance machines, with two and four salient poles, and the modelling of the composite or zebra motor. The results are shown for both conventional and superconductive designs. Finally, the main conclusions made are presented.

## 2. HTS Materials Properties

Superconductivity was discovered in 1911 by Heike Kammerlingh Onnes in Leiden University when Mercury was cooled below 4.2 K. Following this discovery a whole range of metals and alloys, that are conductors at normal temperatures, were found to have similar properties. Superconductivity of the so-called Type I superconductors is modelled by the BCS theory which relies upon the coupling of electron pairs to lattice vibration interactions. However, materials with low resistivity at room temperature do not become superconductors at all. Type I superconductors have found very few practical applications because the critical magnetic fields are relatively small and the required cooling could only be achieved using liquid Helium, an expensive option.

The major breakthrough in superconductivity occurred in

1986 when Alex Müller and George Bednorz, researchers at the IBM Research Laboratory in Switzerland, created a compound of Lanthanum, Barium, Copper and Oxygen, with a perovskite structure that became a superconductor at a temperature of 30 K [2]. In 1987 a research team at the University of Alabama-Huntsville substituted Yttrium for Lanthanum and achieved a critical temperature of 92 K [3]. This was the first time a material ($YBa_2Cu_3O_7$, also referred to as YBCO) had been found to be superconducting at temperatures higher than liquid nitrogen - a cheap and commonly available coolant. Since then, many different ceramics have been found to exhibit superconducting properties. Type-II superconductors usually exist in a mixed state of normal and superconducting regions. This is sometimes called a vortex state, because vortices of superconducting currents surround filaments or cores of normal material. As their critical temperatures are approached, the normal cores become more closely packed. As the superconducting state is eventually lost, they overlap [4].

Type II-Superconductors have the ability to carry large current densities in the order of approximately $10^4$ A/mm$^2$ under no external field, which is much higher than a standard copper wire. These super-currents can therefore be realised in small superconducting segments without any dissipation and consequently such devices can be smaller, as well as offering significant energy savings, when compared to conventional motors. The great disadvantage of Type-II materials is their fragile nature, which makes them difficult to fabricate. When using HTS materials in motors, the design should be done with extreme care to minimize mechanical stresses in these delicate materials. However, when they are suitably combined with other materials, they can become very durable.

## 3. Finite Element Modelling

In the literature, a number of Finite Element modelling tools for electric machines can be found that deal with HTS materials. However, none of them have yet been developed to cope with three-dimensional problems, mainly due to the vast computational effort that is associated with the properties of superconductors. For some very simple cases with suitable geometry and uniform applied fields, analytical solutions can be derived [5,6]. The requirements for a modelling tool that can deal with any motor design are to use the conventional techniques for normal materials, such as iron and current sources, and additionally account for the characteristics of the superconductors. These are demagnetisation and the tendency of these materials to adjust their current distribution to counter-balance changes in the external field. Furthermore, complex geometries of the motor and variable fields in both space and time should be accounted for. The latter is a very important when modelling hysteresis pre-magnetized and trapped field synchronous motors.

The majority of Finite Element Modelling tools that have been developed make use of numerical procedures to deal with multiple materials of arbitrary shape in order to generate field and current distributions [7-12]. The final solution is derived from an iterative procedure that minimizes an energy function of the appropriate form subject to constraints imposed by boundary conditions, continuity equations and properties of the superconductive materials. The main difference between these models is in the iterative procedure that is used for the minimization of the energy function, where gradient descent algorithms and simulated annealing techniques have been proposed.

For the purposes of this study, the Finite Element Modelling tool that was derived at the Department of Engineering of the Oxford University is used. The main points of the developed algorithm are summarized below, but are explained in detail in reference [13]. It consists of two principle parts: The magnetic field solution, which is calculated using conventional techniques, and the current distribution in the superconducting segments, which is determined using Lenz law together with the critical state model of the type II HTS material. Time is handled using a finite difference approximation, making the treatment of the problem magnetostatically. Thermal effects are not considered as well as the operating temperature of the motor.

The quantity to be minimized is an energy factorial that is an integral function of the magnetic vector potential with adjustable parameters. The principle of the finite elements technique is to discretise the domain into a network of nodal points. In each of the constructed elements, the field and current distributions are estimated using an interpolation technique. Finally, the field distribution is obtained from the solution to a set of linear equations. The boundary conditions are set through a recursive ballooning algorithm, which adds the least number of additional layers in an effort to keep the computational time to a minimum.

Some general considerations about the design and material properties were noted throughout the structure of the examined HTS machines. Materials such as iron are considered to have linear properties and are modelled with high values of relative permeability. This approximation is valid only for low magnetic fields sufficiently far from magnetic saturation. The induced critical current in the superconductors was assumed constant, and not varying with temperature and external fields. All models were constructed with a stator of identical geometry with equal magnetic motive force.

An obvious result of the stator design is that the external field does not play any crucial role in the analysis of the motors. The variable of the analysis is the shielding parameter s, estimated as the inverse of the penetration parameter $k$

$$s = \frac{1}{k} = \frac{\mu_o J_c R}{B_o} \quad , \qquad (1)$$

where $J_c$ is the critical current density of the superconductor, $R$ the rotor radius and $B_o$ the external field at the centre of the rotor. This dimensionless parameter presents an indication about the depth of the

superconducting material that is penetrated from the external field. The machines are tested for two different shielding values, namely $s = 2$ and $s = 20$, which correspond to two extreme cases of external field penetration into the superconducting domain.

## 4. Reluctance Machines

Reluctance machines have been widely used in many commercial applications because they are simple to construct and are very robust [14]. Figure 1 shows a view of a conventional reluctance rotor and figure 2 illustrates

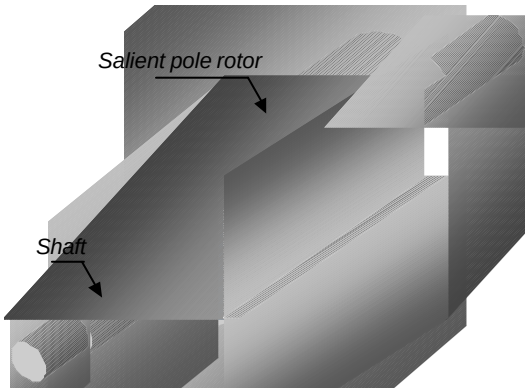


**Figure 1 – Conventional two pole reluctance rotor**

the flux plot of the complete motor. The operating principle of a reluctance machine is to direct the magnetic flux through a specified axis of the rotor. In conventional machines, this is achieved using an iron piece. Two axes can be considered. The first along the direction of the iron, called the direct axis, with low reluctance. The second perpendicular to the first, called the quadrature axis, with high reluctance.

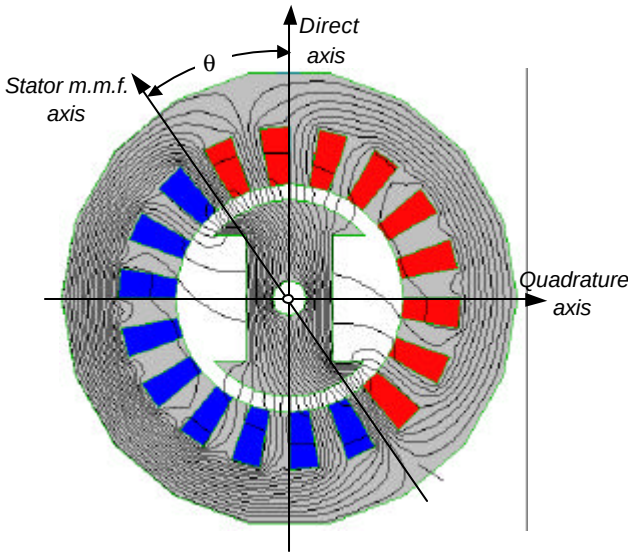


**Figure 2 - Flux plot of a reluctance machine**

The torque in a reluctance machine becomes a function of the torque angle θ [15] according to the equation

$$T(\theta) = \frac{3}{2}\frac{U^2}{\omega^2 L_{max} L_{min}}(L_{max} - L_{min}) sin\, 2\theta \qquad (2)$$

Equation (2) is valid for a three-phase motor fed with constant r.m.s. voltage $U$, and angular frequency $w$. The parameter $L_{max}$ is the maximum stator winding inductance, attained when the rotor longitudinal axis is aligned with the stator magnetic axis ($q = 0$). When the rotor transverse axis is perpendicular with the stator magnetic axis, the stator inductance attains the minimum value $L_{min}$. The torque characteristic of this configuration is improved when the difference ($L_{max} - L_{min}$) is maximized. In conventional reluctance machines, this difference is amplified by increasing the transversal axis reluctance by flanking the rotor with flux barriers [15].

## 5. Reluctance Machine with HTS Materials

A new concept for improving the performance characteristics of reluctance machines is the introduction of HTS materials in the rotor. The diamagnetic properties of superconducting materials are exploited, which prevent magnetic flux from penetrating their surface. A suitable placement of these materials can increase the torque generated by directing the flux solely along the direct axis.

For the reluctance motor, a block of bulk HTS material can easily be fixed to the sides of the salient pole rotor, as shown in figure 3. This HTS material and iron configuration has a very durable structure, in contrast to the brittle nature of stand-alone superconducting materials. Furthermore, it is easier to construct single pieces of the material due to its simple sliced shape. This single piece structure has the extra advantage, compared to a multiple piece HTS, of preventing flux leakage between joints of the various parts.

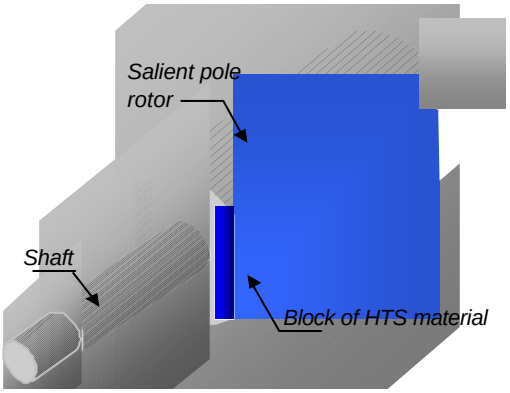


**Figure 3 - Reluctance machine with HTS pieces**

So far, reluctance machines with HTS materials of up to 20kW have been constructed and tested. An initial comparison between conventional machines and those with HTS parts proved somewhat unsatisfactory, as only a small performance improvement was exhibited [16]. In contrast, Barnes predicts an improvement of over 60% in torque production, derived using finite elements analysis [17]. The failure of the prototype machines was attributed

to poor material fabrication at the time of construction.
Two different configurations are presented for the two different values of the shielding parameter s. Initially, the superconducting pieces are considered independent from each other. The corresponding flux plots are displayed in figure 4.

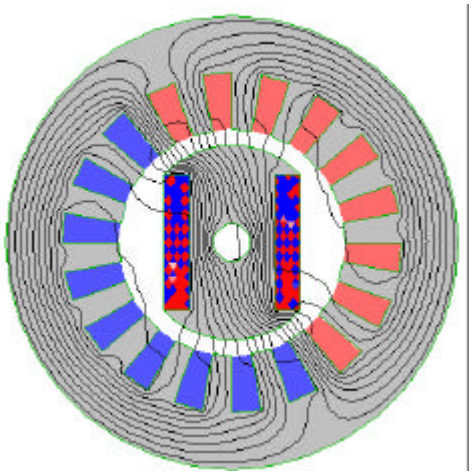

*a) Shielding factor s = 2*

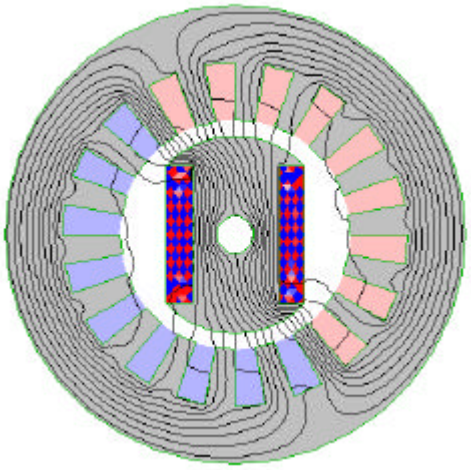

*b) Shielding factor s = 20*

**Figure 4 - Flux plot of the HTS reluctance motor**

The two plots demonstrate the influence that the introduction of a single domain HTS material has on the operational characteristics of the reluctance. The magnetic field, which results from the stator current, $J_{sc}$, results in the induction of a current in the superconducting segment that flows perpendicular to the surface of the material. This acts to repel the magnetic flux from the area of the superconductor. Figures 4(a) and (b) show the influence that the shielding parameter has on the flux. A higher shielding parameter, s, which is equivalent to the higher critical current $J_c$ to stator current $J_{sc}$ ratio, results in fewer flux lines passing through the material.
The flux modelling revealed that on the HTS pieces two areas of similar currents are formed on opposite sites of the salient rotor. These appear to cover a smaller portion of the superconductor surface, which is concentrated towards the end-points of the domain, when the shielding parameter takes a higher value. As expected the amount of flux which transverses the HTS material is significantly reduced for the HTS case.
The second system that was examined assumes an electrical connection between the two superconducting domains, as shown in figure 5. The induced electric current in the superconducting segment is additionally directed between the two superconducting pieces. Thus,

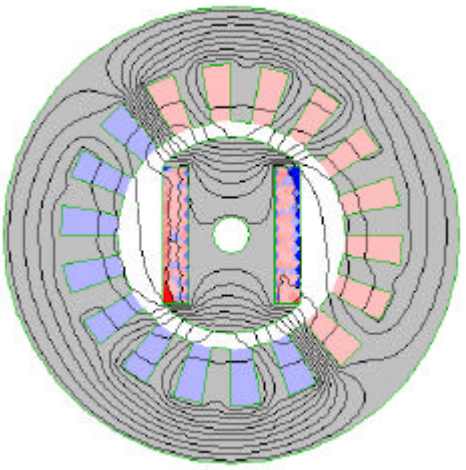

**Figure 5 - Flux plot of the reluctance motor with electrical joined HTS material**
*Shielding factor s ~20*

the resulting field resembles that of two opposing magnetic poles opposing the flux movement through the direct axis of the machine. The flux distribution shows that there is less flux which transverses the superconducting material from the quadrature axis compared to the previous configuration with independent pieces.

## 6. Four - Pole Machine with HTS Materials

A second variation of the previously designed machine consists of the rotor configuration with four salient poles. The conventional machine, shown in figure 6, is

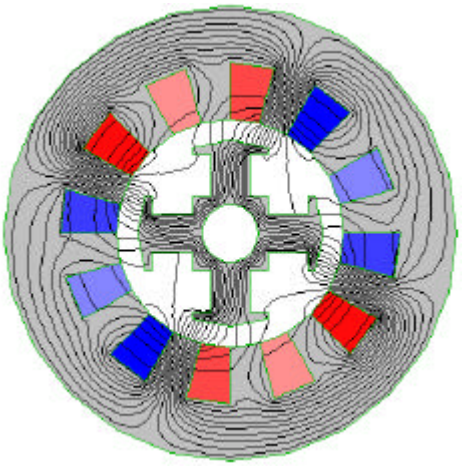

**Figure 6 - Flux plot of a four- pole conventional reluctance machine**

designed to have a suitable space for the introduction of slice shaped HTS segments. The conventional theory for reluctance machines estimates that the produced torque for the four-pole machine is double compared to the two-pole machine.

Experimental four-pole superconducting motors have been developed [16,18,19] and tested but with moderate success, again due to the poor quality of the utilized HTS materials.

Figures 7(a) and 6(b) present plots showing the flux and current distribution of the four-pole motor with different

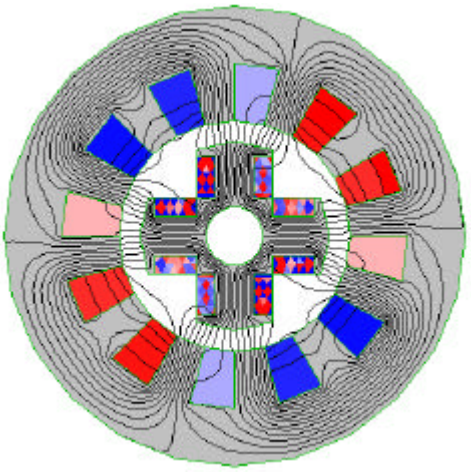

*a) Shielding factor s = 2*

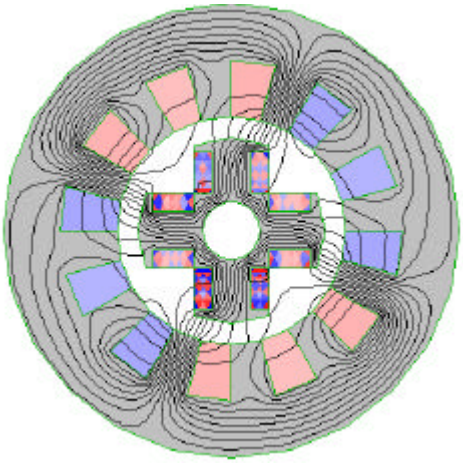

*b) Shielding factor s = 20*

**Figure 7 - Flux plot of a four- pole HTS reluctance machine**

values of the shielding parameter s. The plots indicate that a reduced amount of flux penetrates the superconductor pieces, which results in an increased torque production. As in the two-pole motor, the induced current in the superconductors is mostly located on the edges of the material.

## 7. "Zebra" Motor

An interesting alternative to the salient pole machine is the composite or "zebra" motor, that consists of iron segments placed in alternating order with non-magnetic material, as shown in figure 8. The operating principle of this motor is similar to the conventional reluctance machine discussed previously. The flux is directed to along the direct axis and a high reluctance value is developed on the quadrature axis [15,17]. This results in a high value of the difference ($L_{max} - L_{min}$), as indicated in equation (2), and thus higher torque values. The torque of the zebra motor is approximately 50% higher compared to the conventional reluctance motor, even for non-superconducting cases. The design of this motor that results in the optimum torque value is when the supercon-

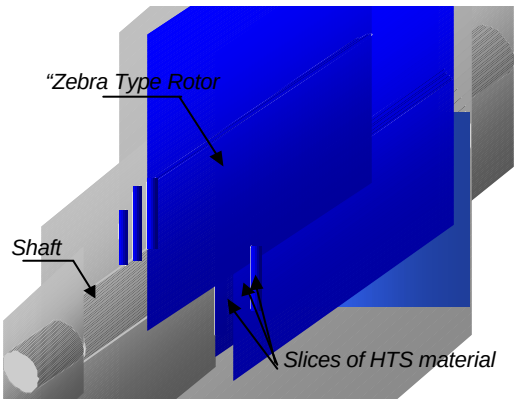


**Figure 8 - "Zebra" rotor**

ducting and iron segments are of the same length. For the purposes of this analysis, all segments were created with equal width, except the middle segment, which contained the shaft. Flux plot for the conventional "zebra" motor, with a shielding factor of s = 0, is shown in figure 9.

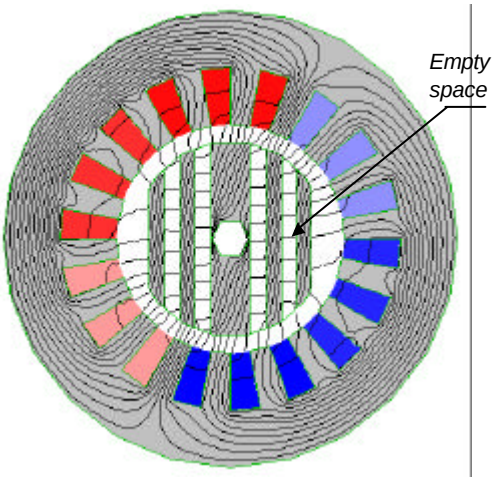


**Figure 9 - Flux plot of a conventional "zebra" type reluctance machine**

*Shielding factor s = 0*

The introduction of superconducting segments between the iron pieces is a new concept for increasing the performance of this machine. Flux plots of this design are generated for two different values of the shielding parameter, s = 2 and s = 20. The corresponding plots are presented in figure 10.

A comparison between figures 9 and 10 clearly demonstrates the effect of the introduction of the superconducting materials. The flux path in the

conventional machine follows the direction of the quadrature axis in the empty segments, is it not completely aligned to the direct axis of the iron pieces. This results in a reduction of the generated torque, as the reluctance difference along the two axes does not take the maximum value. The introduction of the HTS segments modifies the fields so that a reduced amount of flux lines transverse these materials and furthermore, the lines on the iron pieces are aligned more to the direct axis. These characteristics become more intense for higher shielding values, which implies higher critical current ($J_c$) for a constant stator current. These characteristics are enhanced for higher shielding values, but the produced torque exhibits an asymptotic increase as was demonstrated by Barnes [17].

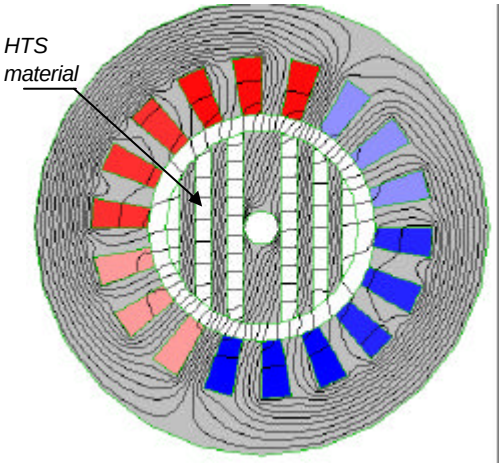


*a) Shielding factor s = 2*

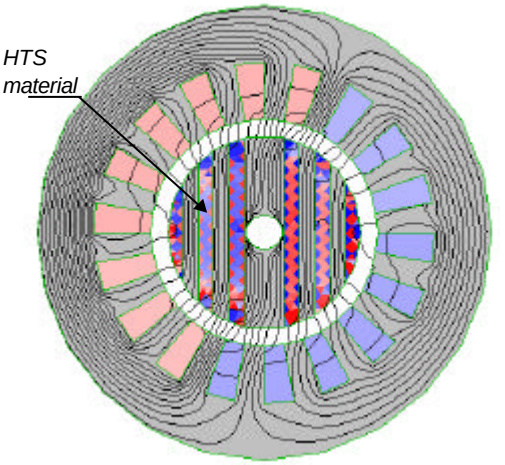


*b) Shielding factor s = 20*

**Figure 10 - Flux plot of a four- pole HTS "zebra" motor**

The finite element modelling of the motor revealed the induced supercurrent to be concentrated towards the boundaries of the HTS segments and an increase of the shielding parameter appears to minimize the area in which higher values of the current can be found. Since the HTS pieces are not electrically joined, the supercurrents are circulating axially in each block.

## 8. Conclusions

This paper examined the flux plot and current distributions of various different reluctance machines that contain bulk pieces of high temperature superconducting material. For this type of motor, the produced torque depends on the difference between the inductance values of the direct and the quadrature axis. A very efficient way of improving the torque production of these machines is the incorporation of HTS segments to act as flux barriers and reduce the amount of flux that transverses the quadrature axis.

Two different types of reluctance motors were examined, the typical machine with two and four poles on the rotor, and the composite or zebra motor. Similar conclusions were found for both designs; the introduction of the HTS material improved the alignment of the flux with the direct axis of the motor, resulting in a greater reluctance difference, ($L_{max} - L_{min}$), and consequently a higher generated torque.

Since type II superconductors do not completely expel magnetic flux from their interiors, the arrangement of the external magnetic field and the operating temperature can actually modify the superconductivity of a Type II superconductor. A decrease in temperature would result in a much greater area of the material exhibiting superconductive properties thus suppressing the space occupied by vortices.

## Acknowledgements

This work was supported by the RTN Supermachines Project nº HPRN-CT-2000-00036. Thanks are also due to the Department of Electrical Engineering of the Faculty of Science and Technology of the New University of Lisbon.

## References

[1] Hoshino T, Muta, I. and Nakamura T., *Applied high-$T_C$ superconducting electrical machines*, Proc of the 2000 KIASC Conference, Taejeon, Korea.

[2] Bednorz, J.G, and Müller K.A., *Possible High $T_C$ Super-conductivity in the Ba-La- Cu- O System*, Z. Phys. B, 64(1986), 1989-1986.

[3] Wu, M.K et al, *High Pressure Study of the New YBCO Superconducting Compound System*, Physical Review Letters, 58(1987), 908.

[4] Tinkham, M., Introduction to Superconductivity, 2nd Ed. McGraw-Hill, 1995.

[5] Mikheenko, P.N. and Kuzovlev, Y.E., *Inductance Mea-surements of HTSC films with high critical currents*, Physica C, 204(1993), 229.

[6] Brandt, E.H. and. Indebom, M., *Type II super-conductor strip with current in a perpendicular magnetic field*, Physics Review B, 48(1993), 12893.

[7] Sanchez, A. and Navau, C., *Current and field penetration in a superconductor in the field of a permanent magnet,* IEEE Tr. On Applied Superconductivity, 9(1999), 1610.

[8] Coombs, T.A. and Campbell, A.M., *A fast algorithm for calculating the critical state in superconductors,* Proc. of the EMF 2000 Conf., Ghent, Belgium.

[9] Prigozhin, L., *Analysis of critical state problems in Type II superconductivity,* IEEE Tr. On Applied Superconductivity, 7(1997), 3866.

[10] Suguira, T., Shashizume, H. and Mika, K., *Numerical electromagnetic field analysis of type II superconductors,* Int J. of Applied Electromagnetics in Materials, 2(1991), 183.

[11] Chun, Y.D., Kim, Y.H., Lee, J, Hong, J.P. and Lee, J.W., *Finite element analysis of magnetic field in high temperature bulk superconductor,* IEEE Tr. On Applied Superconductivity, 11(2001), 2000.

[12] Mashlouh, M, Bouillault, F., Bossavit, A. and Verite, J.C., *From Bean's model to the H-M characteristic of the superconductor: some numerical experiments,* IEEE Tr. On Applied Superconductivity, 7(1997), 3797.

[13] Barnes, G, McCulloch, M. and Dew-Hughes, D., *Computer modelling of type II superconductors in applications,* Superconductor Science and Technology, 12(1999), 518.

[14] Miller, T.J.E., *Switched reluctance motors and their control,* Oxford Science Publications, 1993.

[15] Rodrigues, A.L., *New electric reluctance motor with bulk superconducting materials on the rotor,* Proc. of the 2001 Int. Aegean Conf. On Electrical Machines and Power Electronics, Kusadasi, Turkey.

[16] Oswald, B., Krone, M., Soll, M., Sraβer. T., Oswald J, Best, K.J., Gawalek, W. and Kovalev, L., *Superconducting reluctance motors with YBCO bulk material,* IEEE Tr. On Applied Superconductivity, 9(1999), 1201.

[17] Barnes, G., *Computational modelling for type II superconductivity and the investigation of high temperature superconducting electric machines,* Ph.D. Thesis, Oxford University, 2001.

[18] Joshi, C.H., Prum, C.B., Schiferl, R.F., and Driscoll, D.I., *Demonstration of synchronous motors using high temperature superconducting coils,* IEEE Tr. On Applied Superconductivity, 5(1995), 968.

[19] Eriksson, J.T., Mikkonen, R., Paasi. J., Perala, R. and Soderlund, L., *A HTS synchronous motor at different operating temperatures,* IEEE Tr. On Applied Superconductivity, 7(1997), 523.

* * *